Journal of Engineering and Sustainable Development
https://jeasd.uomustansiriyah.edu.iq/index.php/jeasd
https://doi.org/10.31272/jeasd.28.1.5

Vol. 28, No. 01, January 2024
ISSN 2520-0917

Original Research

TRIPLE-BAND CIRCULAR PATCH MICROSTRIP ANTENNA FOR WIRELESS COMMUNICATION

Abeer Khalid Nghaimesh[*,1], Ali Khalid Jassim[2]

[1,2] *Electrical Engineering Department, College of Engineering, Mustansiriyah University, Baghdad, Iraq*
[1]https://orcid.org/0000-0002-1790-7317
[2]https://orcid.org/0000-0002-4146-4536

Received 04/06/2022 ***Revised 15/08/2022*** ***Accepted 23/12/2023***

Abstract: In this article, a triple-band patch antenna using a circular patch microstrip antenna is constructed with a low-profile patch antenna using a 1.5 mm thick FR4 substrate (εr= 4.3). As mobile devices like smartphones and laptops become more common, the usage of tiny, triple-band antennas has also become more common. The objective of this research is to design a circular patch antenna with a 3–11 GHz dipole-like radiation pattern, which may be used for industrial, scientific, and medical reasons. For the suggested triple-band antenna design, the slotted radiator with six arches and the reduction of the ground plane are among the components. In addition, the standard 50 Ω RF transmission line stimulates the patch antenna; this transmission line is attached to the microstrip line by an impedance-compliant SMA connection. Data from the experiments are obtained, evaluated, and compared; to the patch's surface current distributions, gain, and radiation patterns. According to the measurements, S11 has an impedance bandwidth in the 5.5 GHz band of less than -10 dB, 6.6 GHz band, and 10.4 GHz band at all frequencies. The superb radiation pattern performance, relatively consistent gain throughout the bands, and practical bandwidths of this antenna make it a good choice for C-band and dual X-band applications.

Keywords: *Triple-band; line feed; gain; microstrip antenna; slit; slot*

1. Introduction

Modern portable wireless communication devices that enable several services running in different frequency bands rely on triple-band antennas as a vital component. [1-5]. Portable communication devices must adhere to certain specifications regarding size, efficiency, and power consumption [1]. To achieve this, both the transmitter and receiver end employ planar and low-profile patch antennas to send and receive electrometric radiations [6].

At the design frequency, the height of a low-profile antenna in the open area is less than one-tenth of a wavelength [7, 8]. Patch antennas are sometimes referred to as low-profile antennas [9, 10]. The key benefits of patch antennas are low manufacturing costs, conformability, low profile, and the ability to operate over a broad variety of frequency bands in harsh environments [11-13]. Due to the propagation of surface waves inside a substrate, their shortcomings include a lack of efficiency [14]. Radiating patches may be square, elliptical, circular, triangular, or any combination of these shapes [15, 16]. Each design has a unique combination of advantages and disadvantages to take into account. To activate the radiating patch, several feeding techniques—including a

Corresponding Author: eema1006@uomustansiriyah.edu.iq

probe, microstrip, aperture, and proximity connected—are combined. [17,18]. The most popular methods are the probe and microstrip feed systems [19].

IEEE 52 ones are used to power the antennae. The proximity-linked feed approach provides the highest bandwidth at the expense of a more complex architecture [20, 21].

The strength and bandwidth of the microstrip patch antenna are constrained, which are two of its key drawbacks. In addition, these qualities are being improved in a variety of ways, including the following: (i) A vast number of patch antennas arranged in an array; (ii) increasing the thickness of the substrate; (iii) Impedance matching is improved by using short pins, plates, and pots; (iv) utilizing substrates with high permittivity; (v) modifying the fundamental patch form; (vi) using multiple layers of substrates, and (vii) incorporating metamaterials (MTM) are all examples of novel approaches [22].

This article suggests a slotted, semicircular patch antenna that is supplied by a microstrip. The substrate comprises a thicker FR4 material that measures 1.5 mm in thickness, as opposed to the previous material. his article suggests a slotted, semicircular patch antenna that is supplied by a microstrip. The substrate comprises a thicker FR4 material that measures 1.5 mm in thickness, as opposed to the previous material. Increases in permittivity result in a narrowing of the bandwidth when the substrate's thickness and the dielectric constant have changed, resulting in altered behavior and operation of the antenna. The antenna is capable of supporting three distinct frequency bands, which are extensively utilized for popular communication services such as C-band and dual X-band, respectively. As a result of the patch antenna's many slots, it can operate on three bands despite being much smaller in overall size than a standard rectangular "microstrip patch antenna. CST Studio suite software" is used to conduct the simulations. The antenna is capable of supporting three distinct frequency bands, which are extensively utilized for popular communication services such as C-band and dual X-band, respectively. As a result of the patch antenna's many slots, it can operate on three bands despite being much smaller in overall size than a standard rectangular "microstrip patch antenna. CST Studio suite software" is used to conduct the simulations.

2. Parameter Study

The proposed design takes its core construction component (radiating element) from a multi-band reference semicircular slotted patch antenna, which serves as a model for the proposed design.

The antenna parameters were calculated using a typical antenna equation. Additionally, the settings are optimized to provide optimal multi-band results. The selection of the substrate fabric is critical for the architecture of the microstrip antenna. The higher the substrate thickness, the wider the bandwidth of the antenna. Increased substrate thickness decreases the wave surface, hence increasing the bandwidth. However, the patch’s enhanced bandwidth might be attributable to floor waves or spurious radiation. As a result, substrate selection is critical when considering antenna arrangement [23, 24].

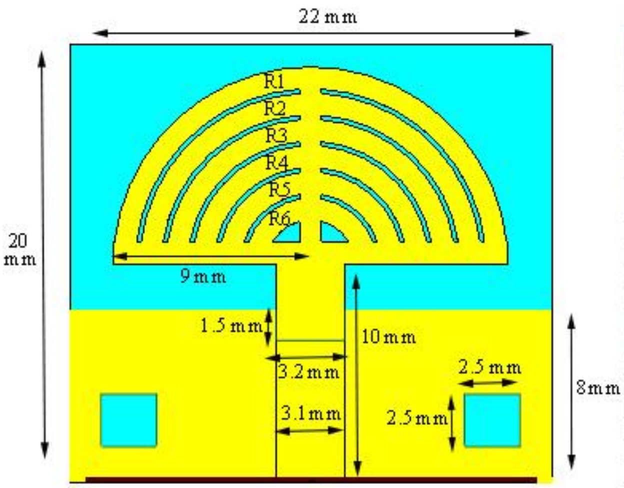

Figure 1. The Triple-Band Antenna's Design

Fig. 1 depicts the proposed antenna form for "Triple-Band applications such as C-band and dual X-band". Table 1 displays the size of the antenna and the crescent-shaped patch. On an FR4 substrate, the antenna measures (20x22x1.5) mm3 and has a relative permittivity (ε_r) of 4.3. CST creates a model of the required form. The width and length of the antenna may be determined using circular patch design equations.

$$f_r = \frac{1.8412_c}{4\pi b_e\sqrt{\varepsilon_r}} \quad (1)$$

$$b_e = b\left(\sqrt{1+\frac{2t}{\pi b\varepsilon_r}\left[ln\left(\frac{\pi b}{2t}+1.7726\right)\right]}\right) \quad (2)$$

Table 1. "Dimensions (mm) of the proposed antenna

parameter	Symbol	Value (mm)"
Width of the ground	Wg	22
Length of the ground	Lg	8
Width of the substrate	Ws	22
Length of the substrate	Ls	20
Width of the feed	Wf	3.1
Length of the feed	Lf	10
Circular radios 1	R1	9
Circular radios 2	R2	7.8
Circular radios 3	R3	6.6
Circular radios 4	R4	5.4
Circular radios 5	R5	4.2
Circular radios 6	R6	3

Using a metallic patch to slit it, as seen in Fig. 2 (a,b,c), leads to a current channel that is significantly longer for a given patch linear dimension. Consequently, reduced greatly is the antenna's fundamental resonant frequency, allowing for significant reductions in antenna area while maintaining a steady operating frequency. In the resonant or excitation direction of the antenna, the resonance frequency is drastically decreased as a consequence of the patch surface current channels being bent, with no lateral current components being generated as a result.

A simulated current distribution across the patch shows how the designed circular slit-cut patch antenna functions, with darker areas denoting higher intensities. Due to the circular patch's slits extending the present path, two more resonances are identified. The resonance frequencies of the extra band may be calculated.

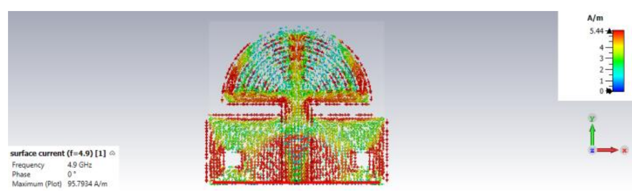

(a) Surface current at 4.9 GHz

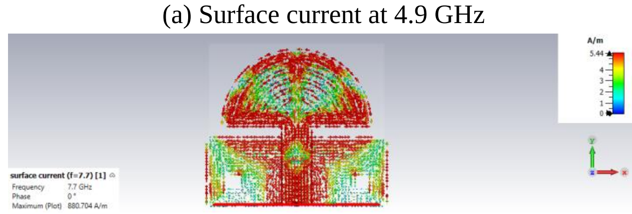

(b) Surface current at 7.7 GHz

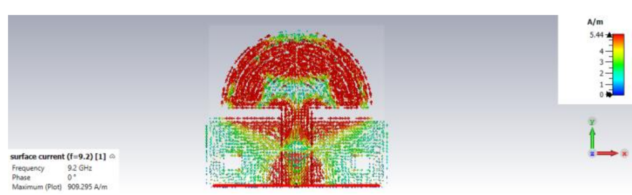

(c) Surface current at 9.2 GHz

Figure 2. Surface current at 4.9 GHz, 7.7 GHz, and 9.2 GHz

3. Effect of Using Different Substrate Materials

The height of the substrate (h), loss tangent (tanδ), dielectric relative constant (ε_r), and width of the feed line (w_f), which are all calculated at 50 ohms, are the main factors affecting changes in bandwidth and surface waves [20-23].

$$\frac{w_f}{h} = \frac{2}{\pi}\left[B - 1 - ln(2B-1) + \frac{\varepsilon_{r-1}}{2\varepsilon_r}\left\{ln(B-1) + 0.39\frac{0.61}{\varepsilon_r}\right\}\right] \quad (3)$$

Where $B = \frac{377\pi}{3Z_o\sqrt{\varepsilon_r}}$ (4)

The equation displays the effective dielectric constant (ε_{eff}) :

$$\varepsilon_{\text{reff}} = \frac{\varepsilon r+1}{2} + \frac{\varepsilon r-1}{2}\left(1 + 12\frac{h}{w}\right)^{-1/2} \quad (5)$$

Since the waves are transmitted via the substrate and the air, the antenna's diameter is used to calculate the causative effects and the degree of fringing.

The CST software program has been used to study and develop a range of dielectric relative constants (ε_r) and thicknesses for a set of materials. The operation and behavior of "the antenna, as well as its effects on variations in substrate thickness and dielectric constant, have all been studied. Increases in (ε_r) result in a narrowing of the bandwidth, an increase in permittivity", a rise in (S_{11}) to a certain point before it starts to decline due to resonance peaks and less than the value at the first peak, and an increase in thickness. Fringing is increased by the substrate, which lowers operating frequency and gain. Furthermore, as indicated in Table 2, changing the material patch at various material types increased the gain and bandwidth constant

Due to their comparable dielectric constants, Arlon AD1000 (ε_r= 10.2), Arlon AD450 (ε_r= 4.5), and FR4 (ε_r= 4.3) are frequently used as substitutes for FR4. In situations when higher frequencies and the possibility for improved fidelity with a wideband signal exceed the performance given, the AD1000 can be utilized in place of FR-4.

Table 2. Gain and reflection coefficient at various frequencies for different materials

Material	Frequency Bandwidth (GHz)	S_{11}	Gain
FR4	4.9	-13	1.7
FR4	7.7	-28	2.5
FR4	9.2	-11	3.2
Arlon AD 450	5.5	-28	2.1
Arlon AD 450	6.5	-21	2.5
Arlon AD 450	10.4	-31	3.1
Arlon AD 1000	5.5	-20	3
Arlon AD 1000	6.6	-37	3.7
Arlon AD 1000	10.4	-28	3.3

However, the manufacture of FR4 panels is extremely inexpensive compared to the other materials, resulting in reduced manufacturing costs overall. Due to the unavailability of Arlon AD1000 (ε_r= 10.2), Arlon AD450 (ε_r= 4.5), FR4 was employed. The S_{11} curves are illustrated in Fig. 3 by altering the substrate materials while maintaining the copper cladding material constant. Arlon AD1000 was determined to be the optimal substrate material since it exhibits three circular polarized bands inside the curve.

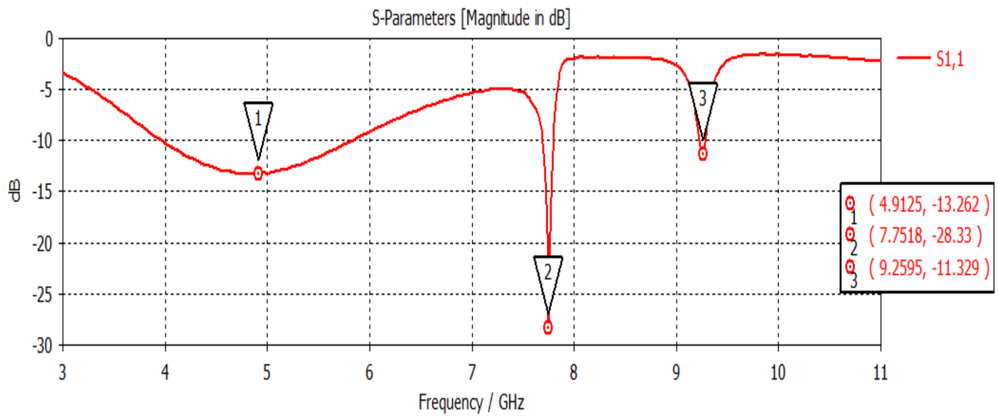

(a) S_{11} for FR4 substrate

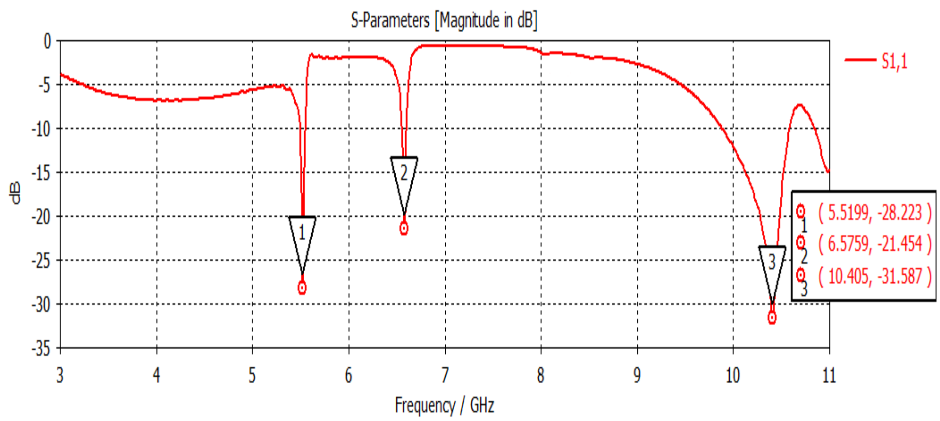

(b) S_{11} for Arlon AD 450 substrate

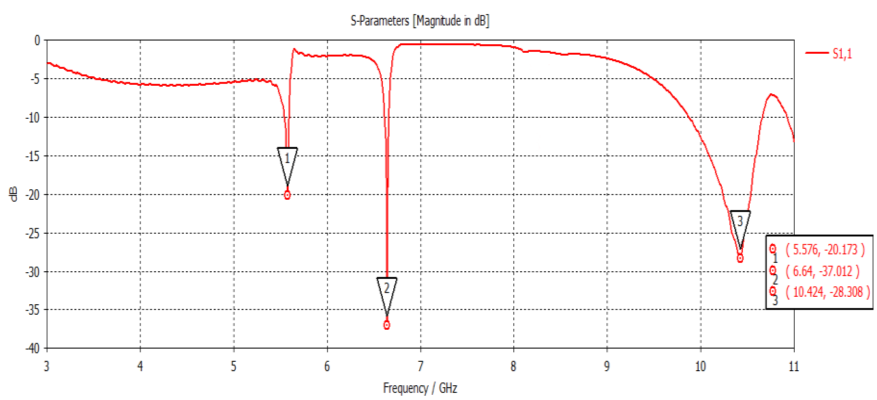

(c) S_{11} for Arlon AD 1000 substrate

Figure 3. S_{11} for FR4, Arlon AD 450 and Arlon AD 1000 substrate

Fig. 4 (a,b,c), illustrates the gain of the antenna.

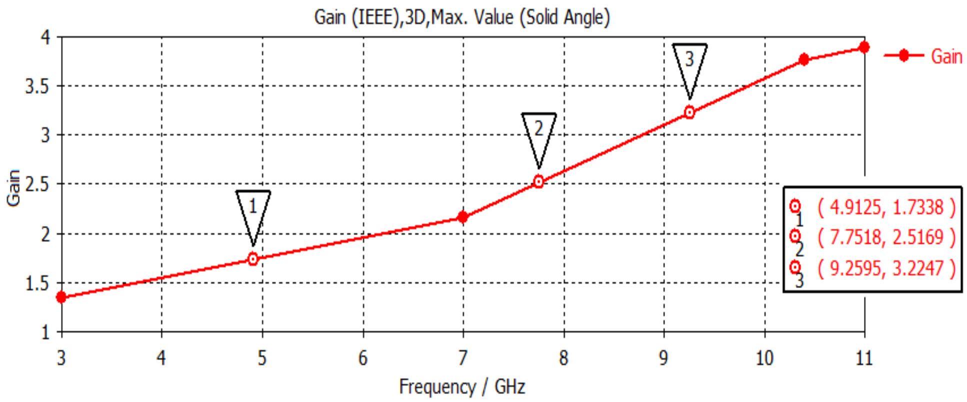

(a) Gain for FR4 substrate

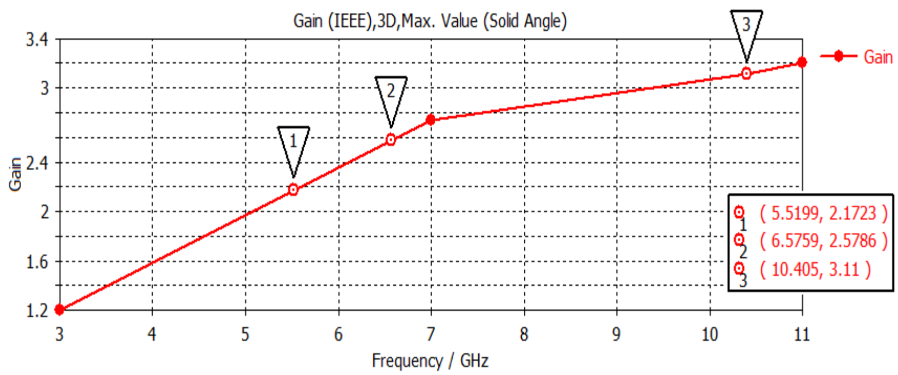

(b) Gain for Arlon AD 450 substrate

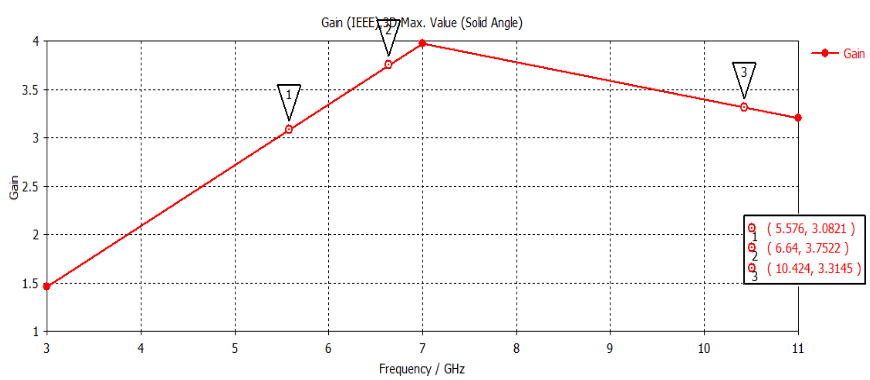

(c) Gain for Arlon AD 1000 substrate

Figure 4. Gain for FR4, Arlon AD 450 and Arlon AD 1000 substrate

4. Results and discussion

The findings are generated after modeling the triple-band antenna. The intended geometry was modeled using CST.

The line-to-load mismatch (defined as the ratio of maximum voltage to minimum voltage or current at any given time) Fig. 5 depicts the voltage standing wave ratio (VSWR).

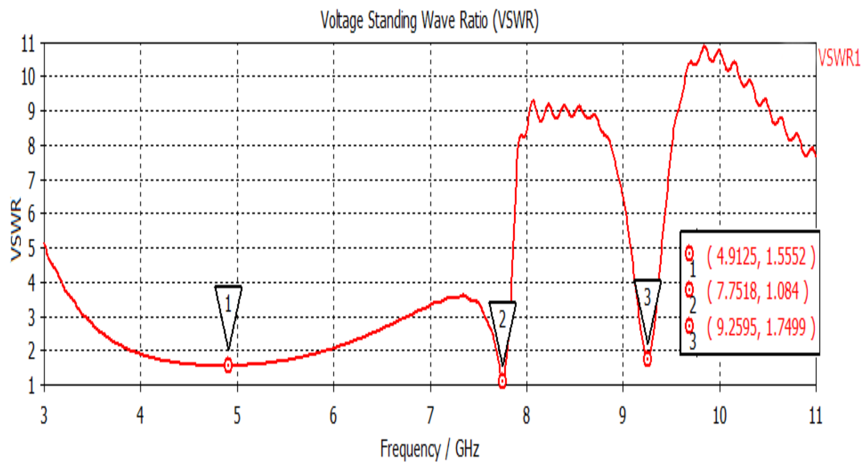

Figure 5. Voltage standing wave ratio at 4.9 GHz, 7.7 GHz, and 9.2 GHz

The far-field broadband gain pattern for the proposed antenna is computed and represented in Fig. 6 as 3.19 dBi, 4.43 dBi, and 4.58 dBi for 4.9 GHz, 7.7 GHz, and 9.2 GHz frequencies, respectively.

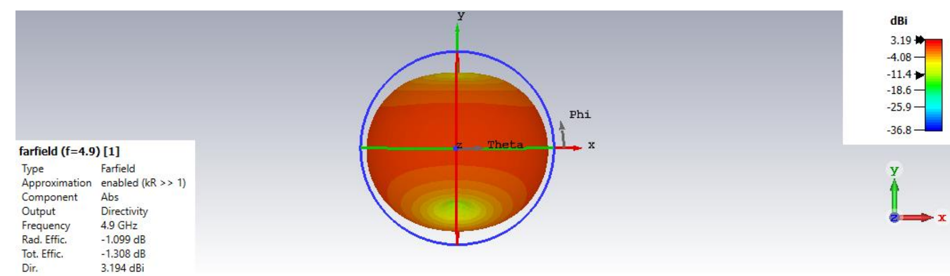

(a) Farfield at 4.9 GHz

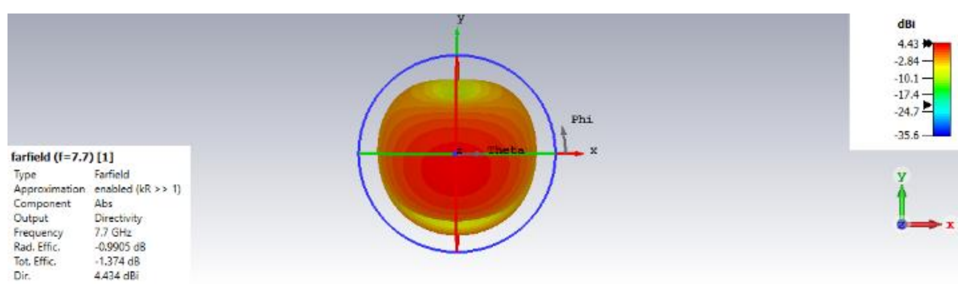

(b) Farfield at 7.7 GHz

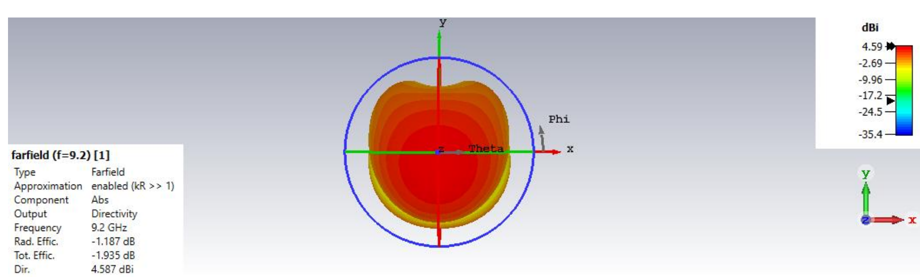

(c) Farfield at 9.2 GHz

Figure 6. Farfield at 4.9 GHz, 7.7 GHz and 9.2 GHz

The antenna has two orthogonal linear polarizations in each of its two planes, allowing for the observation of almost omnidirectional patterns with good separation in both axes (X and Y) as shown in Fig. 7.

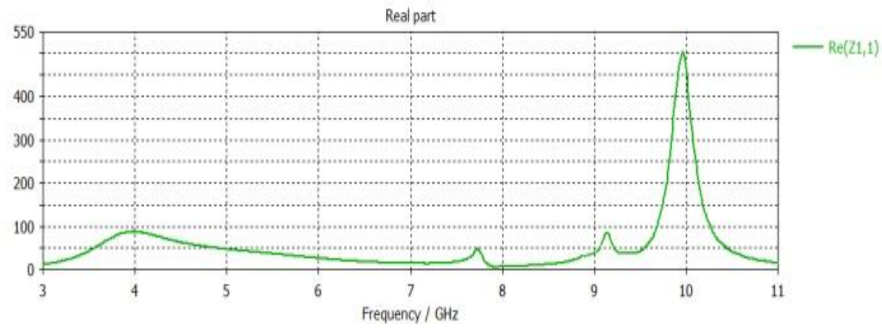

(a) The real impedance value at 4.9 GHz, 7.7 GHz, and 9.2 GHz

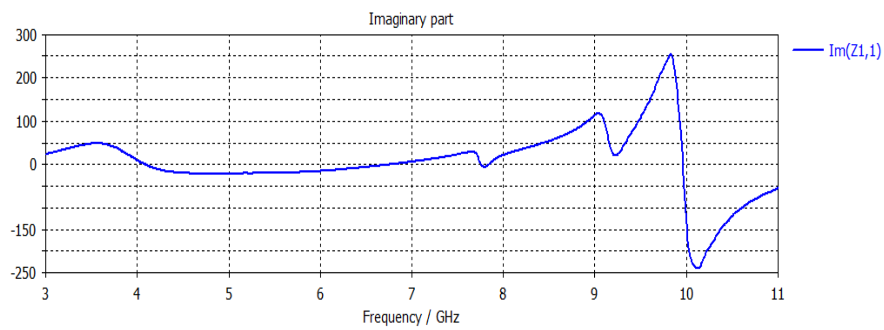

(b) The imaginary impedance value at 4.9 GHz, 7.7 GHz, and 9.2 GHz

Figure 7. The real impedance value and the imaginary impedance value at 4.9 GHz, 7.7 GHz, and 9.2 GHz

5. Conclusions

This study has been conducted to better understand how antenna behavior and operation affect substrate thickness variation and dielectric constant. It is concluded that increases in (ε_r) cause the bandwidth to be narrower. In addition, an increase in permittivity leads to a rise (S_{11}) to a certain amount, then begins to drop owing to resonance peaks. Furthermore, it increases thickness and becomes less than the original peak value. The size of the suggested antenna may be decreased by fabricating it from a different substrate material. The triple-band C-band and dual-band X-band antennas were developed and successfully simulated using the CST studio suite software. The substrate enhances fringing, lowering the operating frequency and decreasing gain. Varying material patches have been studied in a variety of material types. The multi-band antenna that resulted was discovered to resonate at 4.9 GHz, 7.7 GHz, and 9.2 GHz. The results were found to apply to C- and X-band applications.

Acknowledgments

The authors thank Mustansiriyah University for their support of scientific research activities.

Conflict of interest

The authors confirm that there is no conflict of interest associated with the publication of this article.

Author Contribution Statement

Both authors proposed the topic and methodology of the research. The first author wrote this research paper. The second author proof reviewed and gave some comments that would show the research at its current value.

References

1. Kim D.-O. and Kim,C.-Y. 2010. *CPW-fed ultra-wideband antenna with triple-band notch function*, Electronics Letters, Vol. 46, Issue. 18, pp. 1246-1248, https://doi.org/10.1049/el.2010.1415.
2. Basil Nassir, R. ., & Khalid Jassim , A. 2022. *Design Of Mimo Antenna For Wireless Communication Applications*. Journal of Engineering and Sustainable Development, Vol. 26, Issue 4, pp:36–43. https://doi.org/10.31272/jeasd.26.4.4
3. Jabbar Tijil, K. 2014. D*esign and Implementation of Programmable Multi Stage Decimation Filter For Wireless Communication Receivers*. Journal of Engineering and Sustainable Development, Vol. 18, Issue 1, pp:116–128. Retrieved from https://jeasd.uomustansiriyah.edu.iq/index.php/jeasd/article/view/854
4. Thaher H., R. 2016. *Design Of Rectangular Microstrip Patch Antenna For Wireless Communication Systems*. Journal of Engineering and Sustainable Development, Vol. 20, Issue 1, pp:90–101. Retrieved from https://jeasd.uomustansiriyah.edu.iq/index.php/jeasd/article/view/635
5. Tawfeeq Abed Sahab, A. 2016. *A Novel (Q-Slot) Multi Band Antenna For Wireless Communications*. Journal of Engineering and Sustainable Development, Vol.20, Issue 4, 12–18. Retrieved from https://jeasd.uomustansiriyah.edu.iq/index.php/jeasd/article/view/649
6. Gupta S. K., Sharma A., Kanaujia B. K., and Pandey G. P., 2014. *Triple band circular patch microstrip antenna with superstrate*, Wireless personal communications, Vol. 77, Issue. 1, pp. 395-410, https://doi.org/10.1007/s11277-013-1512-2.
7. Saraswat R. K., Dubey S., Singh K. Jeet, Sharma N., and Kachhawa V., 2018. *Design of multi-band octagonal shape patch antenna for WLAN/WIMAX applications*, in *8th International Conference on Communication Systems and Network Technologies (CSNT) 2018*, pp. 21-24, https://doi.org/10.1109/CSNT.2018.8820286.
8. Sharma M., 2020. *Design and analysis of multiband antenna for wireless communication*, Wireless Personal Communications, Vol. 114, Issue. 2, pp. 1389-1402, https://doi.org/10.1007/s11277-020-07425-9.
9. Jassim A. K. and Thaher R. H., 2018. *Design and analysis of broadband elliptical microstrip patch antenna for wireless communication*, TELKOMNIKA Telecommunication Computing Electronics, and Control, Vol. 16, Issue. 6, pp. 2492-2499, https://doi.org/10.12928/telkomnika.v16i6.9246.

10. Osman A., A. 2012. *New Fractal Geometry for Dual Band and Small Size Microstrip Patch Antenna*. Journal of Engineering and Sustainable Development, Vol. 16, Issue 3, 118–125. Retrieved from https://jeasd.uomustansiriyah.edu.iq/index.php/jeasd/article/view/1272

11. Chen W.-F., Yu D., and Gong S.-X., 2015. *An omnidirectional triple-band circular patch antenna based on open elliptical-ring slots and the shorting vias*, Progress In Electromagnetics Research, Vol. 150, pp. 197-203, https://doi.org/10.2528/PIER15010201.

12. Dhara R. and Mitra M., 2020. *A triple-band circularly polarized annular ring antenna with asymmetric ground plane for wireless applications*, Engineering Reports, Vol.. 2, Issue. 4, pp. e12150, https://doi.org/10.1002/eng2.12150.

13. Kamil A. Q. and Jassim A. K. 2021. *Design Of Ultra-Wideband Antenna With Notched Bands To Rejecting Unwanted Bandwidth*, Journal of Engineering and Sustainable Development (JEASD), Vol. 25, Issue. Special_ Issue_2021, https://doi.org/10.31272/jeasd.conf.2.1.20.

14. Falade O. P., Rehman M. U., Gao Y., Chen X., and Parini C. G., 2012. *Single Feed Stacked Patch Circular Polarized Antenna For Triple Band GPS Receivers*, IEEE Transactions on antennas and propagation, Vol. 60, Issue. 10, pp. 4479-4484, https://doi.org/10.1109/TAP.2012.2207354.

15. Raval F., Kosta Y., and Joshi H., 2014. *Triple-band Circular Patch Antenna Using Rising Sun Shaped Metamaterial Structure*, International Journal of Applied Electromagnetics and Mechanics, Vol. 46, Issue. 3, pp. 501-509, https://doi.org/10.3233/JAE-141934.

16. Dildar H. et al., 2020. *Design And Experimental Analysis Of Multiband Frequency Reconfigurable Antenna for 5G and sub-6 GHz Wireless Communication*, Micromachines, Vol. 12, Issue. 1, p. 32, https://doi.org/10.3390/mi12010032.

17. Parveen T., Khan Q. U., Fazal D., Ali U., and Akhtar N., 2019. *Design and Analysis Of Triple Band Circular Patch Antenna*, AEU-International Journal of Electronics and Communications, Vol. 112, pp. 152960, https://doi.org/10.1016/j.aeue.2019.152960.

18. Saxena N. and Rajawat A., 2018. *Design and Analysis of Multi Band antenna for S and C Band*, in International Conference on Advances in Computing: Communication Control and Networking, (ICACCCN) 2018. pp. 894-898, https://doi.org/10.1109/ICACCCN.2018.8748427.

19. Rhazi, Y., El Bakkali, O., Bri, S., Lafkih, M. A., El Mrabet, Y., Nejdi, I. H., & Srifi, M. N., 2018. *Design and Analysis of a Novel Multiband Microstrip Patch Antenna for Wireless Communication*, in International Symposium on Advanced Electrical and Communication Technologies, (ISAECT) 2018. pp. 1-5, https://doi.org/10.1109/ISAECT.2018.8618828.

20. Jassim A. K. and Thaher R. H., 2019. *Calculate The Optimum Slot Area Of The Elliptical Microstrip Antenna For Mobile Applications*, Indonesian Journal of Electrical Engineering and Computer Science, Vol. 16, Issue. 3, pp. 1364-1370, https://doi.org/10.11591/ijeecs.v16.i3. pp.1364-1370.

21. Prasanna M., Rakesh V., and Ahmed M. R., 2018. *Design of Dual-band Microstrip antenna for WiMax and X band applications*, in Second International Conference on Green Computing and Internet of Things, (ICGCIoT) 2018. pp. 598-602, https://doi.org/10.1109/ICGCIoT.2018.8753080.

22. Hamad E. K. and Abdelaziz A., 2019. *Performance of A Metamaterial-Based 1× 2 Microstrip Patch Antenna Array For Wireless Communications Examined By Characteristic Mode Analysis*, Radioengineering, Vol. 28, Issue. 4, p. 681, https://doi.org/10.13164/re.2019.0680.

23. Ahsan M. R., Islam M. T., and Ullah M. H., 2016. *Design and Performance Analysis Of Small-Sized Multiband Microstrip Patch Antenna On Custom-Made Biopolymer Substrate*, Science and Engineering of Composite Materials, Vol. 23, Issue. 6, pp. 729-735, https://doi.org/10.1515/secm-2014-0409.

24. Hussain, M., Jarchavi, S. M. R., Naqvi, S. I., Gulzar, U., Khan, S., Alibakhshikenari, M., & Huynen, I, 2021. *Design and Fabrication of a Printed Tri-Band Antenna for 5G Applications Operating across Ka-, and V-Band Spectrums*, Electronics, Vol. 10, Issue. 21, pp. 2674, https://doi.org/10.3390/electronics10212674.

25. Wei K., Li, J.-Y. Wang L., Z. Xing, and Xu R., 2015. *Study of Multi-Band Circularly Polarized Microstrip Antenna With Compact Size*, Progress In Electromagnetics Research C, Vol. 58, pp. 11-19, https://doi.org/10.2528/PIERC15042905.

26. Ferrero F., Luxey C., Jacquemod G., and Staraj R., 2005. *Dual-band Circularly Polarized Microstrip Antenna For Satellite Applications*, IEEE Antennas, and Wireless Propagation Letters, Vol. 4, pp. 13-15, https://doi.org/10.1109/LAWP.2004.841622.

27. Salih R. M. and Jassim A. K., 2021. *Design And Analysis Of Microstrip Antenna Using Metasurface For Wireless Communication Applications*, Journal of Engineering and Sustainable Development (JEASD), Vol. 25, Special_ Issue_2021, https://doi.org/10.31272/jeasd.conf.2.1.19.

28. Elwi T. A. D. Jassim A., and Mohammed H. H., 2020. *Novel Miniaturized Folded Uwb Microstrip Antenna-Based Metamaterial For Rf Energy Harvesting*, International Journal of Communication Systems, Vol. 33, Issue. 6, p. e4305, https://doi.org/10.1002/dac.4305.